ACS APPLIED MATERIALS & INTERFACES

Research Article

www.acsami.org

Fabrication of a Flexible UV Band-Pass Filter Using Surface Plasmon Metal–Polymer Nanocomposite Films for Promising Laser Applications

Garima Kedawat,*[,†] Bipin Kumar Gupta,*[,‡] Pawan Kumar,[‡] Jaya Dwivedi,[‡] Arun Kumar,[‡] Narendra Kumar Agrawal,[Ψ] Sampath Satheesh Kumar,[⊥] and Yogesh K. Vijay[†]

[†]Department of Physics, University of Rajasthan, Jaipur 302055, India

[‡]CSIR - National Physical Laboratory, Dr K S Krishnan Road, New Delhi 110012, India

[Ψ]Department of Physics, Malaviya National Institute of Technology, Jaipur, Rajasthan-302017, India

[⊥]WITec GmbH, Lise-Meitner-Str. 6, D-89081 Ulm, Germany

Supporting Information

ABSTRACT: We introduce a strategy for the fabrication of silver/polycarbonate (Ag/PC) nanocomposite flexible films of (20 ± 0.01) μm thickness with different filling factor of surface plasmon metal using customized solution cast–thermal evaporation method. Structural characterizations confirmed the good crystallinity with cubic phase of Ag nanoparticles in PC films. Moreover, the microstructural evolutions of nanocomposite films are investigated by transmission electron microscopy, which indicates that the metal fraction is in the form of fractals. Additionally, the surface plasmonic behavior of nanocomposite films has been explored in detail to examine the distribution of Ag nanoparticles in PC film by spectroscopic technique. Furthermore, the obtained transmittance spectral features of this nanocomposite film are suitable for the applications of band-pass filter at 320 nm UV range, which is highly desirable for a HeCd laser.

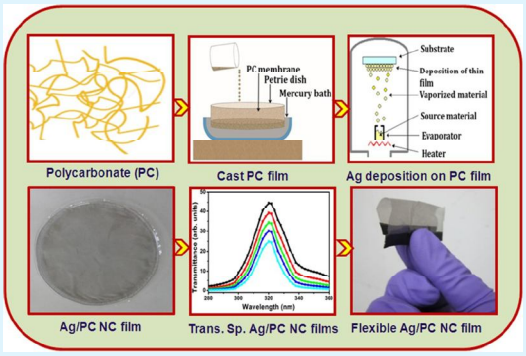

KEYWORDS: *silver nanoparticles, polycarbonate, X–ray diffraction, UV–vis spectroscopy, UV band-pass filter*

INTRODUCTION

Recently, the polymer composite materials based on incorporation of noble inorganic nanoparticles (NPs) provide a potential solution to meet the requirement of present and forthcoming technological demand in virtue of the good processability, structural flexibility, and thermal, mechanical, and optical properties of polymers combined with the unique properties (electrical, optical, and dielectric) of the NPs.[1] The polymer embedded nanostructures have eminent use for a number of technological applications, especially as advanced functional materials, viz., high-energy radiation shielding materials, microwave absorbers, optical filters, reflectors, optical limiters, polarizers, and sensors.[1−3] Thus, the incorporation of inorganic NPs in the polymer system significantly increases the physical parameter range beyond that of the host polymer and allows the material properties for the explicit applications. In particular, the optical properties of polymer nanocomposite (NC) films have huge interest for optoelectronics and photonics devices.[4−6] The properties of polymer NC films depend on the size, shape, and concentration of incorporated NPs and their interaction with the polymer films.[7−9] Incorporation of NPs inside the polymer system provides flexibility and stability. Additionally, polymer encapsulation systems help in preventing both oxidation and aggregation of NPs.

Among the various metals NPs, silver (Ag) metal NPs are of significant interest in a wide field of applications such as catalysts,[10] bactericides,[11] linear or nonlinear optical materials,[12] surface plasmon resonance (SPR) in the UV range,[8] and the ability to modify the refractive index of host materials.[13] The insertion of Ag NPs into polymer films offers considerable interest for environmental protection and allows the plasmonic devices to exploit the mechanical flexibility of polymers and simultaneously prevent the agglomeration of NPs. These are used in photovoltaics,[14] solvent switchable electronic properties,[15] optical limiters or filters,[12,16] surface plasmon enhanced random lasing media,[17] catalytic additives,[18] and antimicrobial coating[19] applications. The central aim of present investigations is focused on the optical applications of nanocomposite films for band-pass filter under the UV range at 320 nm wavelength, which is highly desired for a HeCd laser.[20−22]

Received: March 5, 2014
Accepted: April 25, 2014
Published: April 25, 2014

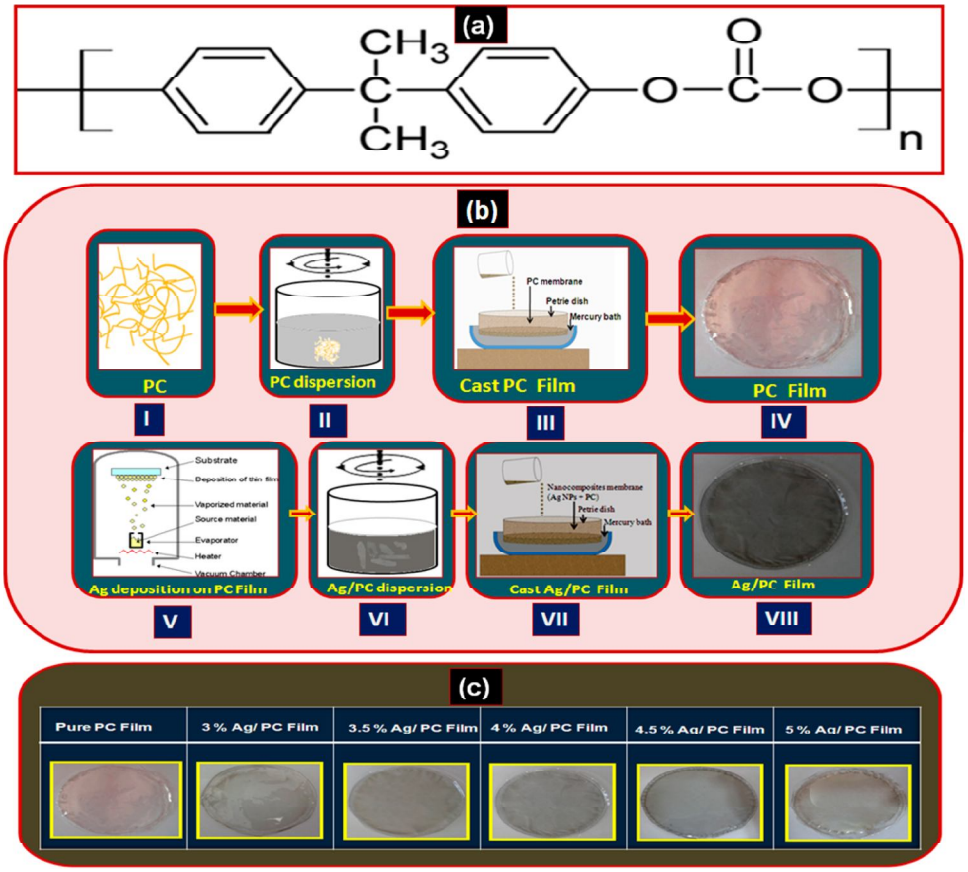

Figure 1. (a) Chemical structure of a repeating unit of polycarbonate. (b) Schematic of indigenously developed process for the fabrication of metal–polymer nanocomposite (Ag/PC NC) films. (c) Photographs of pure PC film and different wt % (3, 3.5, 4, 4.5, and 5) of Ag NPs in PC films.

There have been several coevaporation and co-sputtering approaches for the fabrication of nanocomposite films.[19,23,24] It has also been observed that their behaviors about linear and nonlinear optical properties are different from the pure polymer films. The formation and growth of Ag NPs in the films is affected by the sticking coefficient of metal atoms during deposition. It is also well-known that the linear optical properties (extinction, absorption, and scattering of light) of nanocomposite films are strongly related to the microstructure of films.[25] The present study is aimed at the fabrication and design of silver/polycarbonate nanocomposite (Ag/PC NC) films using customized solution cast–thermal evaporation technique. Polycarbonate (PC) is an optically transparent amorphous thermoplastic resin possessing very low electrical conductivity and has a wide range of useful properties like excellent toughness, flexibility, and very good dimensional as well as thermal stability.[26] The chemical structure of a repeating unit of PC is shown in Figure 1a. The influences of different filling factor of Ag NPs in PC films in terms of composite morphology and optical properties are analyzed and explored in detail in the present study. The obtained results show that such fabricated NC films have suitable application characteristics for band-pass filter under the UV range around 320 nm (a very important wavelength region in laser technology).

■ EXPERIMENTAL SECTION

Synthesis of Ag/PC Nanocomposite Films. The Ag/PC NC films were prepared using customized solution cast followed by thermal evaporation technique. However, polycarbonate [bisphenol A carbonate-*co*-4,4′-(3,3,5-trimethylcyclohexylidene) diphenol] (Aldrich), also known as amorphous polycarbonate (APC), and silver (Ted Pella) were used to fabricate nanolaminate samples[27] and Ag nanoparticle impregnated polycarbonate substrates[28] which have been reported earlier. Initially, 0.169 g of PC was dissolved in 30 mL of dichloromethane (CH_2Cl_2) under magnetic stirrer for 5–6 h. The solution was poured in a flat bottom Petri dish, which was further floating over the mercury bath for 24 h. During this process, the solvent evaporated and film was peeled off and dried in a desiccator under rotary vacuum (10^{-2} Torr) to remove the solvent completely. Thus, PC films of uniform thickness (20 ± 0.01) μm were prepared by customized solution cast method. After that, the Ag NPs with different wt % were deposited on PC films by thermal evaporation technique under high vacuum. The Ag wire (99.99% purity with 1 mm diameter) was wrapped on tungsten filament for the deposition process. The deposition rate was kept precisely about (3.00 ± 0.01) Å/s. The different wt % of Ag NPs deposition on PC films was optimized by the thickness monitor. Further, the Ag deposited PC films were crushed and dissolved in CH_2Cl_2 solution by ultrasonication method for uniform dispersion of Ag NPs in PC polymer. The nanocomposite films were obtained by casting the homogeneous solution in a Petri dish floating on mercury. Thus, the Ag/PC NC films of uniform thickness (20 ± 0.01) μm with different weight fractions (3, 3.5, 4, 4.5, and 5 wt %) of Ag were prepared. The films were dried under vacuum to eliminate the residual solvent. The nanocomposite films were studied in terms of their structural and optical properties. The schematic of complete fabrication process of Ag/PC nanocomposite films is shown in Figure 1b. The photographs of all as-prepared Ag/PC NC films with different weight fractions (3, 3.5, 4, 4.5, and 5 wt %) of Ag NPs are presented in Figure 1c.

Characterization of Ag/PC Nanocomposite Films. The gross structural properties of synthesized Ag/PC NC films were studied

using the X-ray diffraction (XRD) patterns, recorded on a PANalytical X'pert PRO X-ray Diffractometer with Cu Kα_1 radiation of λ = 1.5404 Å wavelength. The distribution of Ag NPs in the polymer films was characterized by high-resolution optical microscopy under transmission mode using Labomed optical microscope at 10× magnification. Scanning electron microscopy (SEM) was performed using Carl ZEISS EVOR-18 equipment at 10 kV operating voltage. For microstructural analysis, transmission electron micrographs (TEM) were obtained by employing a model JEOL — 2000FX operated at voltages of 200 kV. The photoluminescence (PL) characterization of NC films was carried out using luminescence spectrometer (Edinburgh, FLSP — 920) with EPL 375 nm picosecond pulsed diode laser as a source of excitation. The PL mapping of NC films was performed by WITech alpha 300R+ Confocal PL microscope system (WITech GnBH, Ulm, Germeny), where 375 nm diode laser was used as a source of excitation. The UV—vis spectra (transmittance and absorbance) of NC films were recorded using the dual beam Hitachi U3300 spectrophotometer in the spectral range 1200—200 nm with different angle of incidence.

■ RESULTS AND DISCUSSION

The gross structural properties of Ag/PC NC films were studied using the X-ray Diffraction (XRD) patterns. Prior to the XRD measurements, the calibration of the diffractometer was done with silicon powder (d_{111} = 3.1353 Å).[29] Figure 2a—c

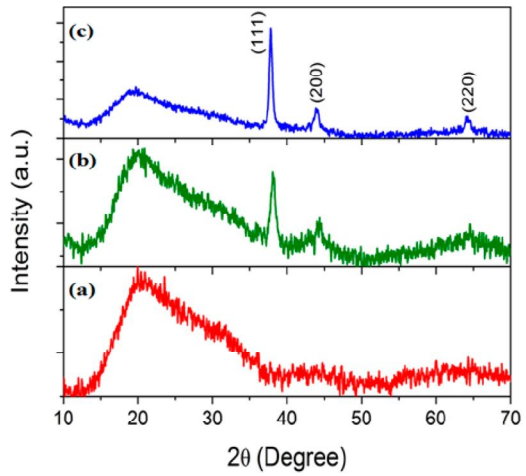

Figure 2. XRD patterns of (a) pure PC film, (b) 3 wt %, and (c) 5 wt % Ag/PC NC film.

exhibit the XRD patterns of pure PC, 3 and 5 wt % Ag/PC NC films. The pure PC is amorphous as expected, and a broad diffraction peak has appeared at about 20.28° which exhibits the signature of PC polymer as shown in Figure 2a. In contrast, the diffraction peaks of 3 and 5 wt % Ag in Ag/PC NC films are shown in Figure 2b and c, respectively. The XRD results reveal that the diffraction peaks of Ag dominate over the polymer amorphous peaks with respect to concentration of Ag nanoparticles in Ag/PC NC films. The diffraction peaks of Ag have face centered cubic (FCC) phase with lattice parameters a = (0.4092 ± 0.012) nm and a = (0.4090 ± 0.023) nm for 3 and 5 wt % Ag in Ag/PC NC films, respectively, which is comparable to the standard value (JCPDS No. 040783, a = 0.4086 nm) as shown in Figure 2b,c. It is interesting to note that a slight shift is observed in major peak of Ag in Ag/PC NC films as shown in Figure 2b,c which depends on the concentration of Ag nanoparticles in Ag/PC NC films. The peaks are indexed as (111), (200), and (220) crystallographic planes corresponding to the 2θ values of 38.239°, 44.265°, and 64.450°, respectively,[30,31] and another broad peak is also observed due to the amorphous PC films. With an increase in wt % of Ag in PC films, the intensity of Ag peaks increases and intensity of PC peaks decreases. The Ag crystalline peaks progressively become sharper and better defined. These results indicate that the intense peaks represent the highly crystalline Ag nanostructures formed in Ag/PC NC films. These dispersed nanocrystallites in the nanocomposite films are also seen by the SEM and TEM images which are further evidenced. However, it is pertinent to note that the appearance of a broad peak (as observed here) is consistent with nanometer-sized crystallites or with a broad range of crystallite size including a nanometer sized fraction.

The optical micrograph images of pure PC films, 3, 4, and 5 wt % Ag/PC NC films are shown in Figure 3a—d. For all the samples, the scale bar is 10 μm. The images show that the distribution of Ag particles throughout the PC films is homogeneous. Thus, this method is the best possible way to acquire a uniform dispersion of the filler inside the polymer matrix which also preserves the properties of Ag NPs.

Scanning electron microscopic (SEM) images of pure PC film and 5 wt % Ag/PC NC film are shown in Figure 4a,b. Both types of samples show homogeneous surfaces. The spots which are marked by red colored circle indicate the presence of nearly spherical clusters of Ag particles and are uniformly dispersed in PC film as shown in Figure 4b. The evidence for the presence of elements in the formation of nanocomposite films based on Ag/PC is given by energy dispersive X-ray spectroscopy (EDS). The spectrum is collected for 5 wt % Ag/PC NC film as shown in Figure 4c. It distinctly indentifies Ag as the elemental component while the other peak belongs to carbon contained in PC film. It also indicates that Ag NPs are well distributed without any chemical and structural modifications into PC film. For further microstructural analysis, transmission electron microscopy (TEM) was performed to evaluate the microstructure information. Figure 5a shows the typical TEM image of 5 wt % Ag/PC NC film. TEM results reveal that Ag NPs are homogeneously dispersed in the PC film and seep in to form an aggregate of irregular shapes. In this case, the NPs are found to be present throughout the entire host matrix of polymer, with the sizes in the range as required for optical applications. The particle size dependent frequency (histogram) is represented in the inset of Figure 5a which shows that the frequency is maximum for the particle size on the order of ∼11 nm. The distance between the particles is very small and the composite is nearly impregnated due to coalescence between the Ag NPs. The elongated uneven shapes of Ag particles are oriented in possible different directions in the PC matrix. The selected area electron diffraction (SAED) pattern for 5 wt % Ag/PC NC film is shown in Figure 5b. It presents a set of rings corresponding to the diffraction from the different planes of nanocrystallites with FCC structure. It is observed that the three rings correspond to the (111), (200), and (220) lattice planes of cubic phase of Ag, which is in good agreement with the XRD results. To evaluate more homogeneous distributions of Ag nanoparticles in 5 wt % Ag/PC NC film, we performed TEM and SAED in different parts of the film as shown in Figures S1—S4 (see Supporting Information). Microstructures of Ag/PC NC film confirm the homogeneous distribution of Ag in PC NC film.

Moreover, it is also interesting to explore as well as track the plasmonic PL signature of Ag/PC NC films by photo-

dx.doi.org/10.1021/am501307h | ACS Appl. Mater. Interfaces 2014, 6, 8407—8414

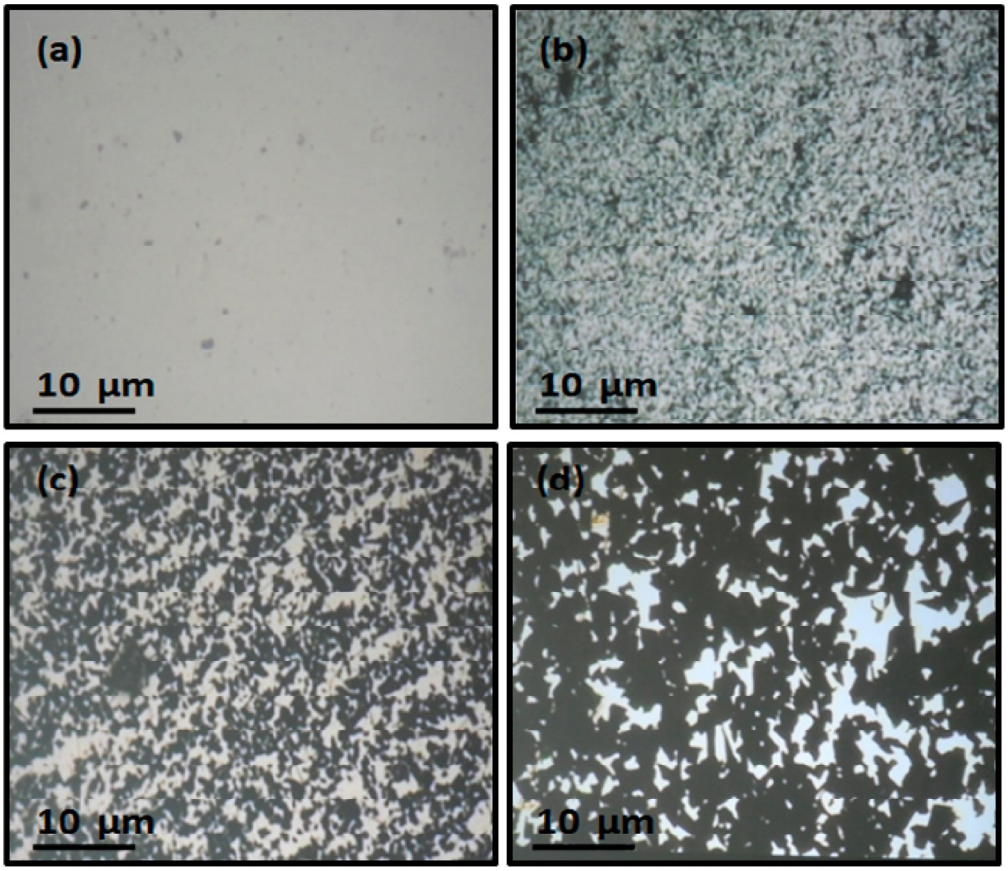

Figure 3. Optical images of (a) pure PC film, (b) 3 wt %, (c) 4 wt %, and (d) 5 wt % Ag/PC NC film.

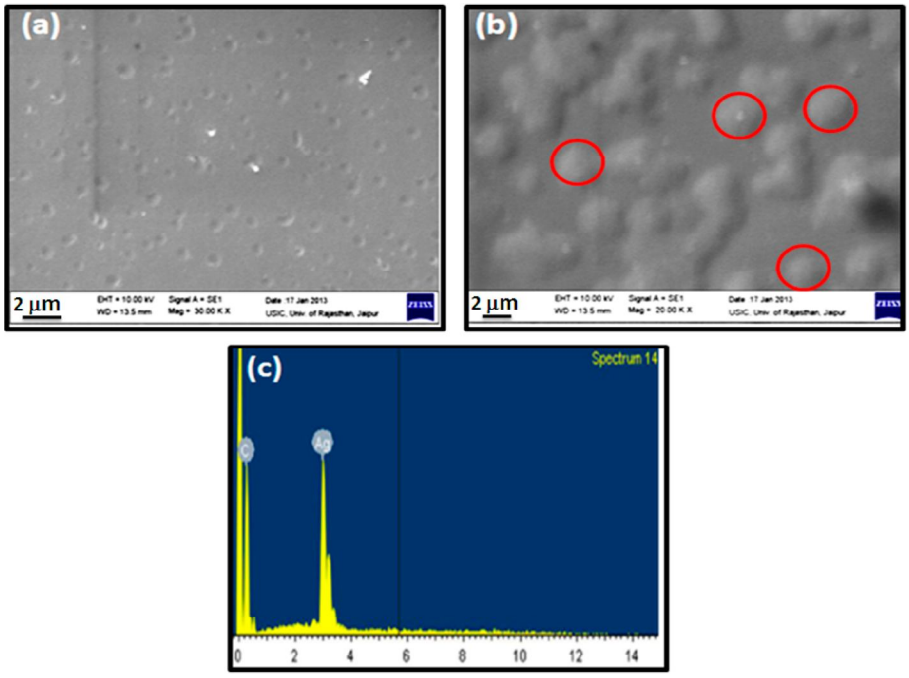

Figure 4. SEM images of (a) pure PC film, (b) 5 wt % Ag/PC NC film, and (c) EDAX spectrum of 5 wt % Ag/PC NC film.

luminescence spectroscopy. Figure 6a,b exhibits the plasmonic photoluminescence emission of Ag nanoparticles in Ag/PC NC films with xenon lamp as source of excitation at 375 nm wavelength. The PL spectra for different wt % (3−5 wt %) of Ag in Ag/PC NC films are shown in Figure 6a. The highest PL emission intensity has been observed for 5 wt % Ag/PC NC

dx.doi.org/10.1021/am501307h | ACS Appl. Mater. Interfaces 2014, 6, 8407−8414

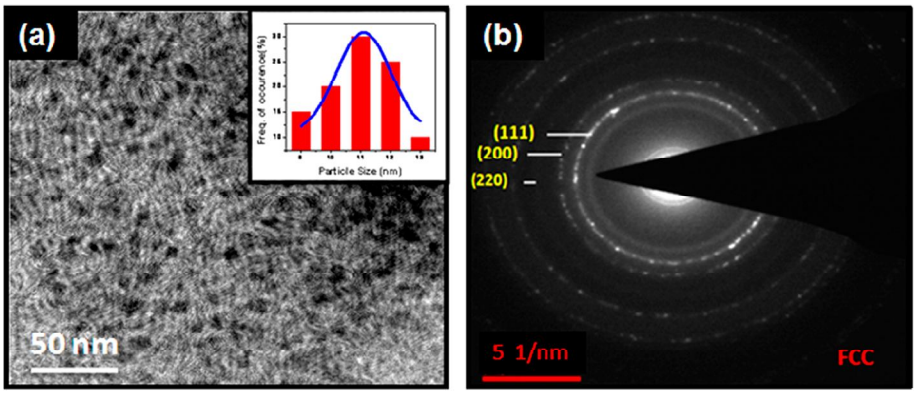

Figure 5. (a) TEM image of 5 wt % Ag/PC NC film and inset shows frequency vs nanoparticles size distribution estimated from TEM image and (b) SAED pattern of 5 wt % Ag/PC NC film.

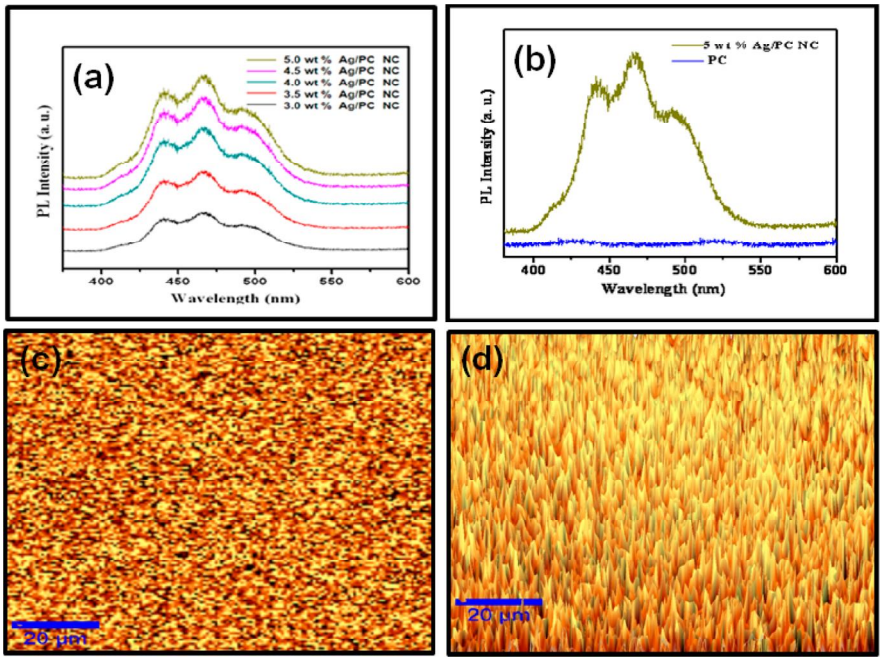

Figure 6. (a) PL spectra of Ag/PC NC films for different wt % (3, 3.5, 4, 4.5, and 5 wt %) of Ag NPs in PC films. (b) PL emission spectra of pure polymer film and optimized wt % (5 wt % Ag) of Ag NPs in PC composite film. (c) 2D view of plasmonic fluorescence PL intensity mapping and (d) 3D lateral view of plasmonic fluorescence PL intensity distribution in Ag/PC NC film.

film. The comparative study of PL emission spectra of pure polymer and optimized 5 wt % Ag/PC NC film is shown in Figure 6b. The PL emission spectra of Ag/PC nanocomposite film is obtained within the visible range, from 380 to 600 nm, with the peak positions at 435, 470, and 495 nm which corresponds to the band to band transition of Ag NPs. It is observed that the intensity of the PL peak increases with the content of silver NPs up to 5 wt %, and beyond it decreases as shown in Figure S5 (Supporting Information). Up to certain concentration of the Ag nanoparticles (2−5 wt %), it is possible to homogeneously disperse Ag nanoparticles in polymer matrix as observed in our experiment; beyond this, homogeneous dispersion of Ag nanoparticles in polymer matrix is difficult. As a result, uneven clustering of Ag is formed in the polymer matrix; thus, the intensity of Ag nanoparticles is quenched at higher concentration (6 wt % and above). Simultaneously, other properties, like absorption, which is required for filter application, are also affected. It is well-known that Ag is a d block element with outer shell electronic configuration $5s^1 4d^{10}$. Thus, the visible plasmonic PL emission of Ag NPs is due to the excitation of electrons from occupied d bands into states above the Fermi level and radiative recombination of an electron with the hole. The optical properties of silver nanoparticles depend on both interband and intraband transitions between electronic states.[32]

Furthermore, we also examine the distribution of silver nanoparticles in Ag/PC NC films by plasmonic PL mapping, which is recorded by confocal PL mapping instrument with a 375 nm diode laser as the source of excitation. The 2D (two-dimensional) view of plasmonic fluorescence mapping and 3D (three-dimensional) lateral view of plasmonic fluorescence distribution in NC film are shown in Figure 6c,d, respectively. The obtained result reveals the uniform distribution of photoluminescence emission intensity in NC films which is attributed from plasmonic emission of Ag NPs. The optical

dx.doi.org/10.1021/am501307h | ACS Appl. Mater. Interfaces 2014, 6, 8407−8414

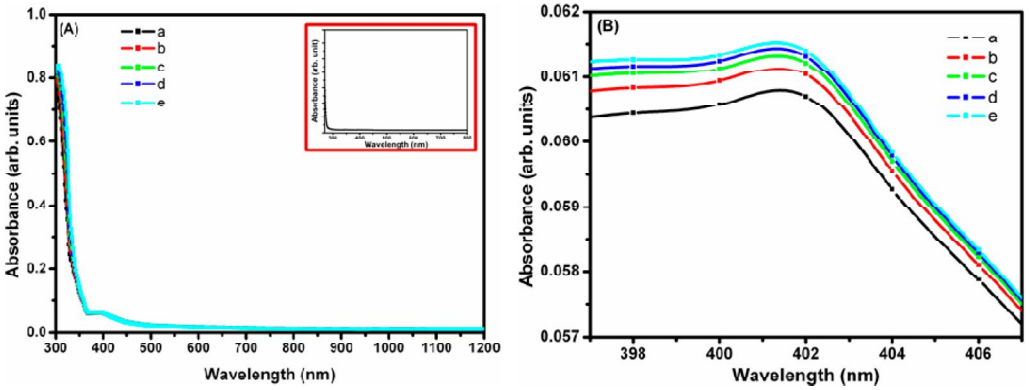

Figure 7. (A) Absorbance spectra for Ag/PC NC films for different wt % of Ag NPs in PC films: (a) 3 wt %, (b) 3.5 wt %, (c) 4 wt %, (d) 4.5 wt %, and (e) 5 wt % Ag/PC NC films; inset shows the absorbance spectra of pure PC films at the normal incidence. (B) Expanded region of the absorbance line width in the range of 397 to 407 nm.

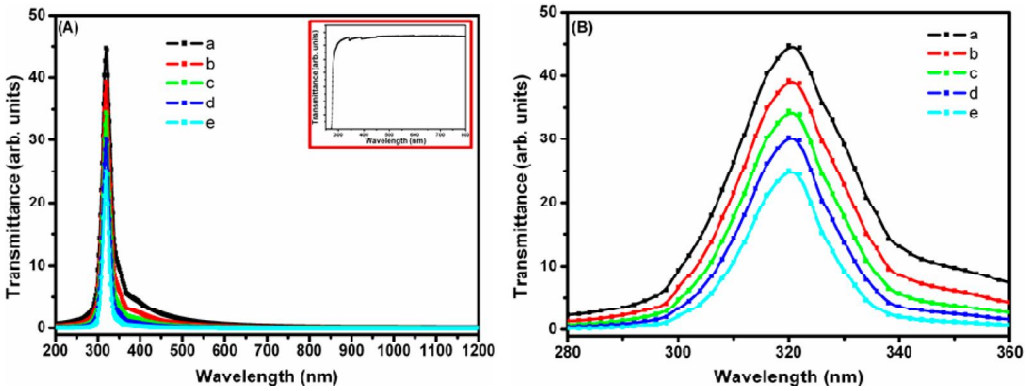

Figure 8. (A) Transmittance spectra for Ag/PC NC films for different wt % of Ag NPs in PC films: (a) 3 wt %, (b) 3.5 wt %, (c) 4 wt %, (d) 4.5 wt %, and (e) 5 wt % Ag/PC NC films; inset shows the transmittance spectra of pure PC films at the normal incidence. (B) Expanded region of the transmittance line width in the range of 280 to 360 nm.

micrograph images of 5 wt % Ag/PC NC film is shown in Figure S6 (Supporting Information).

UV–vis absorption spectra are shown in Figure 7A for different wt % of Ag NPs in PC films and the inset shows the absorbance spectra of pure PC film at the normal incidence. The absorbance spectra reveal that there is no absorbance of pure PC film before the addition of Ag NPs, while broad SPR bands are found at around 401 nm for NC systems due to excitation of the surface plasmon vibrations or interband transitions of Ag atoms dispersed in the PC matrix, which indicates the formation of Ag NPs (clearly shown in Figure 7B). This is in agreement with the calculations based on Mie scattering theory. The width of the observed SPR peaks for the composite system might be due to the size distribution of silver NPs. The intensity and broadening of the peak increases with the wt % of Ag NPs, and peaks are very minorly shifted to the lower wavelength, indicating that mean diameters of Ag NPs have increased.

The transmittance spectra of Ag/PC NC films for different wt % of Ag NPs in PC films are shown in Figure 8A and the inset shows the transmittance spectra of the pure PC film. It reveals two interesting features. First, it shows the narrow band transmittance around 320 nm wavelength and the block the rest of the spectrum (400–1200 nm) that has significant interest, being the same wavelength as that of the HeCd laser. The maximum transmittance wavelength at $\lambda \approx 320$ nm is mainly due to the interplay between the end of the absorption edge of the polymer and the beginning of the surface plasmon resonance absorption band edge of silver. Second, the width of the transmittance band varies with Ag contents. With an increase the concentration of Ag in the polycarbonate matrix, the bandwidth becomes narrower and the attenuation of transmittance intensity increases at 320 nm wavelength. These effects are clearly seen in Figure 8B which represents the expanded region of corresponding transmittance line width in the range of 280 to 360 nm. The narrow band is a result of the combined composition of PC polymer at the lower wavelength and Ag nanostructure at the higher wavelength region, which is the lower wavelength edge of the broad plasmon resonance of the Ag nanostructures.[33] The variation of full width at half-maximum (fwhm) and corresponding transmittance with the wt % of Ag NPs in PC films is summarized in Table 1. This shows that the distribution of Ag NPs in PC films affects the

Table 1. Variation of fwhm and Transmittance for Different wt% of Ag/PC NC Films

sample	Ag (wt %)	fwhm (nm)	transmittance (%)
a	3	25	44
b	3.5	23	39
c	4	20	34
d	4.5	19	30
e	5	17	25

dx.doi.org/10.1021/am501307h | ACS Appl. Mater. Interfaces 2014, 6, 8407–8414

transmissivity, which was not previously reported for the Ag/PC nanocomposite system to the best of our knowledge. Additionally, by tilting the fabricated filters in the present case, the angle of incidence varies from 0° to 70°; a blue shift is observed in the transmittance peak for 5 wt % Ag/PC NC film as shown in Figure 9 and results are summarized in Table 2.

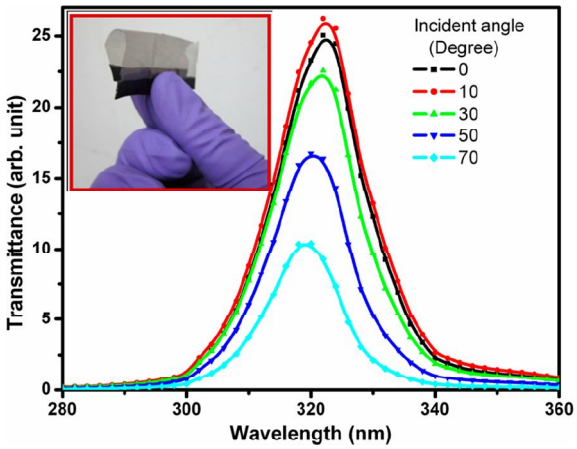

Figure 9. Transmittance spectra for 5 wt % Ag/PC NC film for different angles of incidence and inset exhibits the flexibility of film.

Table 2. Transmittance as a Function of Angle of Incidence for 5 wt % Ag/PC NC Film

angle (deg)	transmittance (%)	peak wavelength (nm)	fwhm (nm)
0	25	320	17
10	23	320	17
30	21	319	16
50	16	318	12
70	11	317	11

These changes occur due to the optical path difference between the waves reflected from either side of the film structure. These changes are also observed for all other samples, as shown in Figures S7–S10 (see Supporting Information). The inset of Figure 9 shows the high flexibility of film after several statistical foldings. It can be folded up to 360° without any kind of distortion in the film. Thus, these Ag/PC nanocomposite films have ultimate optical properties with flexibility, which is highly desired for the fabrication of HeCd laser as a band-pass filter at 320 nm UV range. Its excellent wavelength is matched to the photopolymer and film sensitivity ranges. HeCd laser is extensively used in 3D stereolithogarphy, printing and typesetting, fluorescence excitation investigations for current scientific research, and holographic applications.

■ CONCLUSION

The strategy to design the various compositions of Ag/PC NC films having (20 ± 0.01) μm thickness using the simple solution cast–thermal evaporation method are demonstrated successfully and described in detail. The fabrication method is simple and effective and can be used for large scale production. The fine dispersion of Ag NPs inside the polymer films was obtained and confirmed through the structural/microstructural analysis of Ag/PC NC films. TEM images suggest the superior crystallinity and cubic phase of Ag NPs in PC films, which are in good agreement with the XRD results. The plasmonic fluorescence mapping attests to the uniform distribution of Ag NPs in Ag/PC NC films. The narrow transmittance at 320 nm arises due to the absorption edge of polymer and metal fractals in the nanocomposite films. The transmittance range is tunable from 44% to 25% at 320 nm by the variation of Ag wt % in PC films. The fwhm is about 17 nm with 25% transmittance for 5 wt % Ag/PC NC films. Furthermore, a blue shift was observed in the transmittance peak with a variation in the angle of incidence from 0° to 70° for 5 wt % Ag/PC NC films. The central wavelength shifts toward the shortwave part and relatively decreases the transmittance as the angle of incidence increases. Thus, these Ag/PC nanocomposite films have specific features to act as a band-pass filter at 320 nm UV range which makes it highly suitable for potential applications with HeCd laser.

■ ASSOCIATED CONTENT

Supporting Information

TEM and SAED of Ag/PC NC films at different parts and PL spectra of various wt % of Ag in Ag/PC NC films. This material is available free of charge via the Internet at http://pubs.acs.org.

■ AUTHOR INFORMATION

Corresponding Authors

*E-mail: kedawat08@gmail.com.
*E-mail: bipinbhu@yahoo.com.

Notes

The authors declare no competing financial interest.

■ ACKNOWLEDGMENTS

The authors wish to thank Prof. R. C. Budhani, Director, N.P.L., New Delhi, for his keen interest in the work. The authors are thankful to Prof. O.N. Srivastava (Banaras Hindu University, Varanasi) for his encouragement. The authors gratefully acknowledged University Grant Commission (UGC) and Council of Scientific and Industrial Research (CSIR), Govt. of India, for financial assistance and Department of Physics, University of Rajasthan, Jaipur (India), for experimental facilities to carry out this work.

■ ABBREVIATIONS

PC, polycarbonate; NPs, nanoparticles; NC, nanocomposite

■ REFERENCES

(1) Nicolais, L.; Carotenuto, G. *Metal-Polymer Nanocomposites*; John Wiley & Sons, Inc.: Hoboken, NJ, 2005.
(2) Judeinstein, P.; Sanchez, C. Hybrid Organic-Inorganic Materials: A Land of Multidisciplinarity. *J. Mater. Chem.* **1996,** *6*, 511–525.
(3) Caseri, W. Nanocomposites of Polymers and Metals or Semiconductors: Historical Background and Optical Properties. *Macromol. Rapid Commun.* **2000,** *2*, 705–722.
(4) Ravirajan, P.; Haque, S. A.; Durrant, J. R.; Bradley, D. D. C.; Nelson, J. The Effect of Polymer Optoelectronics Properties on the Performance of Multilayer Hybrid Polymer/TiO_2 Solar cells. *Adv. Funct. Mater.* **2005,** *15*, 609–618.
(5) Zaman, S.; Zainelabdin, A.; Amin, G.; Nur, O.; Willander, M. Effect of the Polymer Emission on the Electroluminescence Characteristics of N-Zno Nanorods/P-Polymer Hybrid Light Emitting Diode. *Appl. Phys. A: Mater. Sci. Process.* **2011,** *104*, 1203–1209.
(6) Firth, A. V.; Haggata, S. W.; Khanna, P. K.; Williams, S. J.; Allen, J. W.; Magennis, S. W.; Samuel, I. D. W.; Cole-Hamilton, D. J. Production and Luminescent Properties of Cdse and Cds Nanoparticle-Polymer Composites. *J. Lumin.* **2004,** *109*, 163–172.

(7) Torigoe, K.; Suzuki, A.; Esumi, K. Au(III)-PAMAM Interaction and Formation of Au-PAMAM Nanocomposites in Ethyl Acetate. *J. Colloid Interface Sci.* **2001,** *241,* 346–356.
(8) Mishra, Y. K.; Mohapatra, S.; Chakravadhanula, V. S. K.; Lalla, N. P.; Zaporojtchenko, V.; Avasthi, D. K.; Faupel, F. Synthesis and Characterization of Ag-Polymer Nanocomposites. *J. Nanosci. Nanotechnol.* **2010,** *10,* 2833–2837.
(9) Pandey, J. K.; Reddy, K. R.; Kumar, A. P.; Singh, R. P. An Overview on the Degradability of Polymer Nanocomposites. *Polym. Degrad. Stab.* **2005,** *88,* 234–250.
(10) Xu, R.; Wang, D.; Zhang, J.; Li, Y. Shape-Dependent Catalytic Activity of Silver Nanoparticles for the Oxidation of Styrene. *Chem.—Asian J.* **2006,** *1,* 888–893.
(11) Maneerung, T.; Tokura, S.; Rujiravanit, R. Impregnation of Silver Nanoparticles into Bacterial Cellulose for Antimicrobial Wound Dressing. *Carbohydr. Polym.* **2008,** *72,* 43–51.
(12) Sun, Y. P.; Riggs, J. E.; Rollins, H. W.; Guduru, R. Strong Optical Limiting of Silver-Containing Nanocrystalline Particles in Stable Suspensions. *J. Phys. Chem. B* **1999,** *103,* 77–82.
(13) Singho, N. D.; Lah, N. A. C.; Johan, M. R.; Ahmad, R. Enhancement of the Refractive Index of Silver Nanoparticles in Poly (Methyl Methacrylate). *Int. J. Res. Eng. Technol.* **2012,** *1,* 231–234.
(14) Chaudhary, V.; Thakur, A. K.; Bhowmick, A. K. Improved Optical and Electrical Response in Metal-Polymer Nanocomposites for Photovoltaic Applications. *J. Mater. Sci.* **2011,** *46,* 6096–6105.
(15) Haes, A. J.; Van Duyne, R. P. A Nanoscale Optical Biosensor: Sensitivity and Selectivity of an Approach Based on the Localized Surface Plasmon Resonance Spectroscopy of Triangular Silver Nanoparticles. *J. Am. Chem. Soc.* **2002,** *124,* 10596–10604.
(16) Dirix, Y.; Bastiaansen, C.; Caseri, W.; Smith, P. Oriented Pearl-Necklace Arrays of Metallic Nanoparticles in Polymers: A New Route toward Polarization-Dependent Color Filters. *Adv. Mater.* **1999,** *11,* 223–227.
(17) Meng, X.; Fujita, K.; Zong, Y.; Murai, S.; Tanaka, K. Random Lasers with Coherent Feedback from Highly Transparent Polymer Films Embedded with Silver Nanoparticles. *Appl. Phys. Lett.* **2008,** *92,* 201112.
(18) Murugadoss, A.; Chattopadhyay, A. A Green Chitosan-Silver Nanoparticles Composite as a Heterogeneous as well as Micro-Heterogeneous Catalyst. *Nanotechnology* **2008,** *19,* 015603.
(19) Lee, S. H.; Sung, K.; Chung, T. M.; Lee, S. G.; Min, K. D.; Koo, S.; Kim, C. G. Preparation of Silver Nanoparticles and Antibiotic Test of Its Polycarbonate Films Composite. *J. Nanosci. Nanotechnol.* **2008,** *8,* 4734–4737.
(20) Bloemer, M. J.; Scalora, M. Transmissive Properties of Ag/MgF_2 Photonic Band Gaps. *Appl. Phys. Lett.* **1998,** *72,* 1676–1678.
(21) Jaksic, Z.; Maksimovic, M.; Sarajlic, M. Silver–Silica Transparent Metal Structures as Bandpass Filters for the Ultraviolet Range. *J. Opt. A: Pure Appl. Opt.* **2005,** *7,* 51–55.
(22) Scalora, M.; Bloemer, M. J.; Pathel, A. S.; Dowling, J. P.; Bowden, C. M.; Manka, A. S. Transparent, Metallo-Dielectric, One-Dimensional, Photonic Band-Gap Structures. *J. Appl. Phys.* **1998,** *83,* 2377–2383.
(23) Singho, N. D.; Lah, N. A. C.; Johan, M. R.; Ahmad, R. FTIR Studies on Silver-Poly(Methylmethacrylate) Nanocomposites via *In-Situ* Polymerization Technique. *Int. J. Electrochem. Sci.* **2012,** *7,* 5596–5603.
(24) Takele, H.; Greve, H.; Pochstein, C.; Zaporojtchenko, V.; Faupel, F. Plasmonic Properties of Ag Nanoclusters in Various Polymer Matrices. *Nanotechnology* **2006,** *17,* 3499–3505.
(25) Heilmann, A.; Werner, J.; Stenzel, O.; Homilius, F. Changes of the Optical and Electrical Properties of Plasma Polymer-Metal Composite Films during Thermal Annealing. *Thin Solid Films* **1994,** *246,* 77–85.
(26) Moreno, I.; Navascues, N.; Irusta, S.; Santamaría, J. Silver Nanowires/Polycarbonate Composites for Conductive Films. *IOP Conf. Ser.: Mater. Sci. Eng.* **2012,** *40,* 012001.
(27) Roberts, M. J.; Feng, S.; Moran, M.; Johnson, L. Effective Permittivity Near Zero in Nanolaminates of Silver and Amorphous Polycarbonate. *J. Nanophotonics* **2010,** *4,* 043511.
(28) Lagonigro, L.; Hasell, T.; Rohrmoser, S.; Howdle, S. M.; Sazio, P. J. A.; Lagoudakis, P. G.; Peacock, A. C. Silver Nanoparticle Impregnated Polycarbonate Substrates for Plasmonic Application. *IEEE-LEOS-Winter Topicals Meeting Series* **2009,** 48–49.
(29) Kedawat, G.; Srivastava, S.; Jain, V. K.; Pawan; Kataria, V.; Agrawal, Y.; Gupta, B.; Vijay, Y. K. Fabrication of Artificially Stacked Ultrathin ZnS/MgF_2 Multilayer Dielectric Optical Filters. *ACS Appl. Mater. Interfaces* **2013,** *5,* 4872–4877.
(30) Jiang, G. H.; Wang, L.; Chen, T.; Yu, H. J.; Wang, J. J. Preparation and Characterization of Dendritic Silver Nanoparticles. *J. Mater. Sci.* **2005,** *40,* 1681–1683.
(31) Temgire, M. K.; Joshi, S. S. Optical and Structural Studies of Silver Nanoparticles. *Radiat. Phys. Chem.* **2004,** *71,* 1039–1044.
(32) Vasireddy, R.; Paul, R.; Mitra, A. K. Green Synthesis of Silver Nanoparticles and the Study of Optical Properties. *Nanomater. Nanotechnol.* **2012,** *2,* 1–6.
(33) Avasthi, D. K.; Mishra, Y. K.; Kabiraj, D.; Lalla, N. P.; Pivin, J. C. Synthesis of Metal–Polymer Nanocomposite for Optical Applications. *Nanotechnology* **2007,** *18,* 125604.